THE JOURNAL OF PHYSICAL CHEMISTRY B

Article

pubs.acs.org/JPCB

Rationalization of the Solvation Effects on the AtO^+ Ground-State Change

Tahra Ayed,[†] Florent Réal,[§] Gilles Montavon,[‡] and Nicolas Galland*[,†]

[†]CEISAM, UMR CNRS 6230, Université de Nantes, 2 Rue de la Houssinière, BP 92208, 44322 Nantes Cedex 3, France

[§]PhLAM, UMR CNRS 8523, Université de Lille 1, Bât. P5, 59655 Villeneuve d'Ascq Cedex, France

[‡]SUBATECH, UMR CNRS 6457, IN2P3/EMN Nantes/Université de Nantes, 4 rue A. Kastler, BP 20722, 44307 Nantes Cedex 3, France

Supporting Information

ABSTRACT: ^{211}At radionuclide is of considerable interest as a radiotherapeutic agent for targeted alpha therapy in nuclear medicine, but major obstacles remain because the basic chemistry of astatine (At) is not well understood. The AtO^+ cationic form might be currently used for ^{211}At-labeling protocols in aqueous solution and has proved to readily react with inorganic/organic ligands. But AtO^+ reactivity must be hindered at first glance by spin restriction quantum rules: the ground state of the free cation has a dominant triplet character. Investigating AtO^+ clustered with an increasing number of water molecules and using various flavors of relativistic quantum methods, we found that AtO^+ adopts in solution a Kramers restricted closed-shell configuration resembling a scalar-relativistic singlet. The ground-state change was traced back to strong interactions, namely, attractive electrostatic interactions and charge transfer, with water molecules of the first solvation shell that lift up the degeneracy of the frontier π^* molecular orbitals (MOs). This peculiarity brings an alternative explanation to the highly variable reproducibility reported for some astatine reactions: depending on the production protocols (with distillation in gas-phase or "wet chemistry" extraction), ^{211}At may or may not readily react.

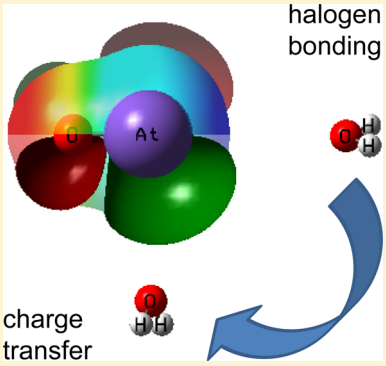

1. INTRODUCTION

Astatine (At), element 85 in the periodic table of elements, is the heaviest naturally occurring halogen. Because it has no stable isotopes, At belongs to the rarest of all elements. One of its longest-lived isotopes, ^{211}At (half-life = 7.21 h), is of considerable interest as a radiotherapeutic agent for the future of targeted alpha therapy in nuclear medicine.[1,2] However, binding At to cancer-selective carrier molecules is a difficult task. Since it was discovered over 70 years ago, many of its characteristics remain elusive. It has been recognized recently that many of the basic chemical studies with At have unfortunately been set aside, which currently hinders the development of radiotherapeutic agents.[3] This work aims specifically at getting a deeper understanding of the astatine basic properties. Considering the available amounts of ^{211}At produced in cyclotrons, 10^{-13} to 10^{-9} g, the theoretical calculations are to date the only tool to gain an insight into this "invisible" element at the molecular level.[4,5]

Unlike the other halogens, At exists in different cationic forms in aqueous solutions that are thermodynamically stable. We have recently identified one predominant form in oxidizing conditions, namely, AtO^+.[6,7] This cationic species might be currently used for the ^{211}At-labeling of carrier biomolecules with boron cage pendant groups[8] if we look closely at the experimental conditions. Very recently, we have pointed out an intriguing behavior of AtO^+ in solution: it reacts with simple inorganic and organic compounds,[4,9−11] while the electronic configuration of the free molecular ion is:

$$(\text{core})^{80}1\sigma^2 1\sigma^{*2} 2\sigma^2 1\pi^4 1\pi^{*2}$$

In a spin−orbit free picture, the ground state is $X^3\Sigma^-$ and the reactions of AtO^+ with most compounds (being usually closed-shell) are expected to be spin-forbidden. Considering the stability of various $AtO^+(H_2O)_6$ clusters, we have shown using relativistic quantum calculations that numerous hydrate clusters with a closed-shell configuration are found to be significantly more stable than the lowest-lying cluster with a triplet configuration.[12] In the present work, we focus our attention at revealing the fundaments of the ground-state change, providing simultaneously a full demonstration of the fact that the solvated AtO^+ is dominated by a Kramers-restricted closed-shell configuration resembling to a scalar-relativistic singlet. We have considered several clusters with AtO^+ and an increasing number of water molecules, $AtO^+(H_2O)_n$ with n = 1−6. The long-range bulk effects on the solute are introduced by means of an implicit solvent model to improve the simulation of the solvation process. Note that because astatine is a heavy-element, spin-free and spin-dependent relativistic effects on the AtO^+ solvation must be investigated. Hence, several flavor of

Received: July 10, 2013
Revised: August 7, 2013
Published: August 14, 2013

relativistic quantum methods have been used on $AtO^+(H_2O)_n$ clusters.

2. COMPUTATIONAL DETAILS

We have followed a computational methodology similar to the one used in our previous investigation of $AtO^+(H_2O)_6$ clusters.[12] For the triplet and singlet electronic configurations, the energies, structures, and vibrational properties of the most stable $AtO^+(H_2O)_n$ clusters have been first determined through unrestricted and restricted density functional theory (DFT) calculations, respectively. Because of its efficiency for accurately predicting (i) singlet−triplet transition energies and (ii) nonbonding interactions including hydrogen bonding, we have selected the recently introduced M06-2X meta hybrid functional.[13,14] We have used the scalar-relativistic ECP60MDF pseudopotential (PP) in conjunction with a modified aug-cc-pVDZ-PP (mAVDZ) basis set for At atom[4,15] and the aug-cc-pVDZ basis sets for H and O atoms.[16,17] When it was required, CASSCF single-point calculations have been carried out using the MOLPRO 2012.1 package[18] to ensure that the wave functions of the studied electronic states can be described by a single determinant, which allows us to apply all of the range of single-reference based methods. Additional single-point energy calculations on the previously DFT optimized structures have been performed using the MP2 and CCSD(T) methods in conjunction with the aug-cc-pVTZ-PP-2c (AVTZ-2c) basis set[19] for At atom and the aug-cc-pVTZ basis sets[16,17] for H and O atoms. For the sake of simplicity, Gibbs free energies calculated using (i) either MP2 or CCSD(T) energies and (ii) M06-2X structural and vibrational properties will be referred to as, respectively, MP2//M06-2X and CCSD(T)//M06-2X throughout the text. The free energy of (i) the full population of the triplet clusters and (ii) the full population of the singlet clusters is estimated according to the following relation:

$$G^o_{\{A\}} = -RT \ln \sum_{i\in\{A\}} e^{-G^o_i/RT}$$

where {A} emphasizes calculation over the population of all A clusters (A being triplet or singlet).

The spin−orbit DFT (SODFT) method available in the NWChem programs package[20] has been successfully used to investigate spin−orbit coupling (SOC) effects on molecules containing astatine.[4−7,21,22] The SODFT method is a two-component (2c) approach that makes use of PPs, like ECP60MDF, which contain scalar and spin-dependent potentials. Therefore, electron correlation and relativistic effects, including SOC, are treated on an equal footing into the variational treatment. Starting from the previous wave functions and structures localized on the triplet and singlet potential energy surfaces, 2c-M06-2X/mAVDZ geometry optimizations have been performed following the SODFT framework. Harmonic vibrational frequencies were evaluated by two-sided finite differences of analytical gradients. On the 2c-M06-2X/mAVDZ optimized structures, single-point energy calculations have been carried out using (i) the above-mentioned PP and triple-ζ basis sets and (ii) the 2c-MP2 method implemented in the TURBOMOLE program package.[19,23] Note that the core electrons were frozen for all post-HF calculations (notably the 5s, 5p, and 5d inner cores of At). For the sake of simplicity, free energies calculated using (i) 2c-MP2/AVTZ-2c energies and (ii) 2c-M06-2X/mAVDZ structural and vibrational properties, will be referred to 2c-(MP2//M06-2X) throughout the text.

Free energies of the clusters in solution were derived by means of a thermodynamic cycle applied to systems in the gas phase, with corrections for solvation energies, as shown in Scheme 1. Therefore, the free-energy difference in solution between singlet and triplet $AtO^+(H_2O)_n$ clusters can be calculated from its components:

$$\Delta G^*_{\text{sing-trip}}(aq) = \Delta G^o_{\text{sing-trip}}(g) + \Delta G^*_{sol}(AtO^+(H_2O)_{n,sing}) - \Delta G^*_{sol}(AtO^+(H_2O)_{n,trip})$$

Scheme 1. Thermodynamic Cycle Applied to the Calculation of the Free Energy Difference in Solution Between the Singlet and Triplet $AtO^+(H_2O)_n$ Clusters

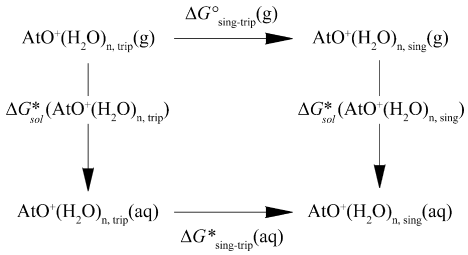

Gibbs free energies of aqueous solvation were computed using the SMD continuum model.[24] However, at present no parameters for At are included in this model. Following the recommendations of Truhlar et al.,[24] we have used the van der Waals radius of astatine, 2.02 Å,[25] to define its cavity. To minimize the influence of At cavity on the computed solvation free energies, the SMD calculations were restrained to the larger $AtO^+(H_2O)_n$ clusters (n = 4−6), where the At atom is crowded by the explicit water molecules. The geometries of the clusters were optimized in the presence of the solvent for computing the solvation free energies. The latter have been determined at M06-2X/mAVDZ level of theory using the Gaussian program package,[26] used as well for all other scalar-relativistic calculations (except when noted).

3. RESULTS AND DISCUSSION

3.1. Where the Ground State Change is Evidenced.

For the free AtO^+ molecular ion, the π^{*2} electronic configuration leads to a degenerated triplet ground state $X^3\Sigma^-$ (the latter is split into $X_1 0^+$ and $X_2 1$ electronic states upon inclusion of SOC) and a first singlet excited state $a^1\Delta$ (denoted $a2$ with SOC), which lies at ∼66 kJ mol^{-1}.[27] The presence of polar molecules creates an external field that surely induces a modification of the electronic structure and the associated state ordering. Thus all of the discussion will focus on the microsolvated cation.

Spin−Orbit Free Calculations. First, we present gas-phase calculations at M06-2X/mAVDZ level of theory for various $AtO^+(H_2O)_n$ clusters to show the relations between the stability and the electronic structure. For $AtO^+(H_2O)$ clusters, the optimization under the C_{2v} symmetry constraint reveals that the singlet and the triplet electronic states correspond, respectively, to a transition state and a minimum (T1 ($^3A_2$) species in Figure 1). Relaxation of the C_{2v} symmetry constraint

dx.doi.org/10.1021/jp406803e | J. Phys. Chem. B 2013, 117, 10589−10595

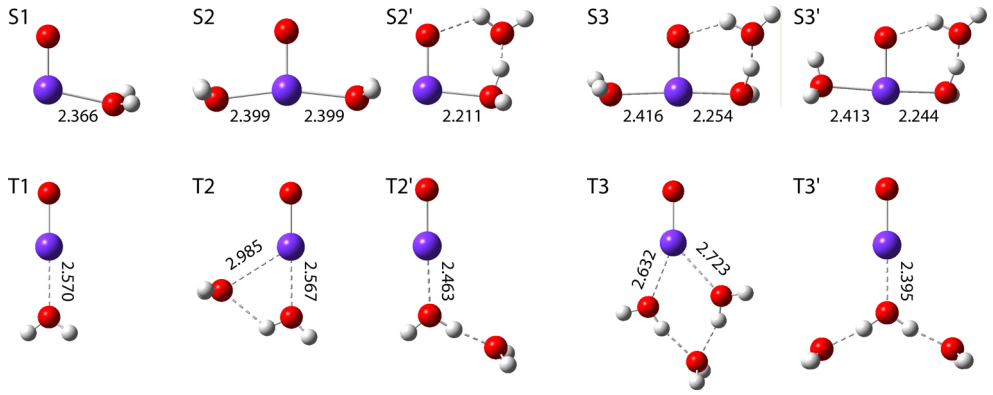

Figure 1. Molecular structures of the two most stable $AtO^+(H_2O)_n$ clusters, n = 1−3, calculated at M06-2X/mAVDZ level of theory for the singlet (top, S index) and triplet (bottom, T index) spin multiplicities. The distances between At and the closest water molecules are given in angstroms. Color code: magenta for At, red for O, and gray for H.

for the singlet state yields a C_s minimum (S1 ($^1A'$) species in Figure 1). The calculated Gibbs free energies show that the triplet structure is more stable than the singlet one by 81.7 kJ mol^{-1}. We have evaluated how the basis set superposition error (BSSE) changes this value. Using the counterpoise methodology with monomer relaxation, we found a trifling increase of 0.2 kJ mol^{-1}. BSSE was neglected in what follows except when noted. Adding one more water molecule leads to new species heavily related to the previous $AtO^+(H_2O)$ clusters. The structures of the singlet species exhibit extremely different patterns from those of the triplets. The most stable one (S2 ($^1A_1$) species in Figure 1) is characterized by two water molecules located almost perpendicularly to the AtO^+ fragment, resulting in a T-shape structure. The geometries issued from the triplet state (T2 ($^3A'$) and T2′ ($^3A'$) species in Figure 1) retain the water molecule that interacts with astatine through an halogen bond, as shown by the linearity (close to 180°) of the interaction between the water oxygen atom and the AtO^+ fragment. In these structures, the second water molecule interacts with the previous one through hydrogen bonds. Note that the triplet species are the most stable. The optimization of $AtO^+(H_2O)_3$ clusters shows structures that are strongly related to the $AtO^+(H_2O)_2$ ones, especially for the singlet clusters: all exhibit T-shape geometries with a water molecule mainly engaged in hydrogen bonds with (i) the oxygen atom of AtO^+ and (ii) a water molecule interacting with astatine. Regarding the structures obtained for the triplet state, the water molecules are essentially connected within a network of hydrogen bonds, which is structured by the water molecule engaged in an halogen bond with At. The M06-2X/mAVDZ calculations show that the free-energy difference between the singlet and triplet clusters has dropped down to 8.1 kJ mol^{-1}.

Figure 2 shows how the free-energy difference between the singlet and triplet $AtO^+(H_2O)_n$ clusters is modified according to the number of explicit water molecules (n = 1−6). Indeed, the difference decreases regularly, and it was found to become negative, −13.3 kJ mol^{-1}, for $AtO^+(H_2O)_4$ clusters. This means that the singlet clusters become more stable than the triplet ones. This result is confirmed for $AtO^+(H_2O)_5$ clusters and the previously studied $AtO^+(H_2O)_6$ clusters.[12] Note that the presence of 4 water molecules around AtO^+ fragment leads to 15 minima and the presence of 5 and 6 water molecules leads, respectively, to 16 and 18 minima. The structures optimized using an implicit solvation model for the two most abundant singlet and triplet $AtO^+(H_2O)_n$ clusters, with n = 4−6, are displayed in Figure 3. These structures are close parents to the ones previously discussed for n = 3. It is essentially the network of water molecules connected by hydrogen bonds that grows. The implicit solvation model (SMD) has been introduced to account for the long-range bulk effects of the solvent. The relative stabilities may be modified for clusters of the same size (same n value) and electronic state. Table 1 reports the computed free-energy difference between the singlet and triplet $AtO^+(H_2O)_n$ clusters when n goes from 4 to 6. The results show that the combined contributions of specific interactions with water molecules of the first solvation shell and bulk effects of the solvent magnify the ground-state change of AtO^+. The singlet clusters are even more stable than the triplet ones, by 38.0 kJ mol^{-1} when four explicit water molecules are considered up to 53.0 kJ mol^{-1} when six explicit water molecules are considered. Note that the same trends can be drawn on the basis of ab initio calculations (see Table S1 in the Supporting Information) and that the choice of a specific implicit model for describing the solvent long-range effects has minor influence, as it was previously shown for $AtO^+(H_2O)_6$ clusters.[12]

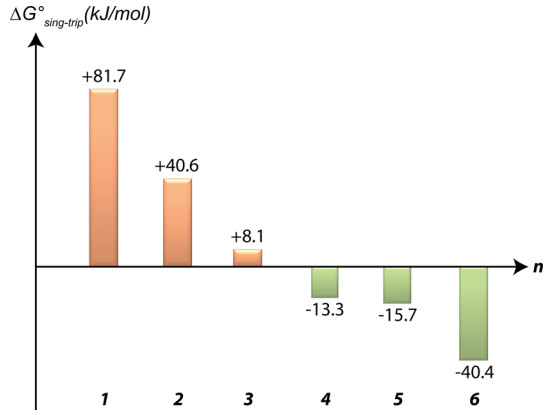

Figure 2. Evolution of the free-energy difference, computed at M06-2X/mAVDZ level of theory, between the singlet and triplet $AtO^+(H_2O)_n$ clusters, with n increasing up to 6.

SOC-Based Calculations. Consideration of relativistic effects is, in general, essential for the theoretical description of molecules that contain heavy elements. It is widely known that the inclusion of spin−orbit interactions are necessary for calculations on heavy p-elements such as At. Previous theoretical investigations have notably shown that AtO^+

dx.doi.org/10.1021/jp406803e | J. Phys. Chem. B 2013, 117, 10589−10595

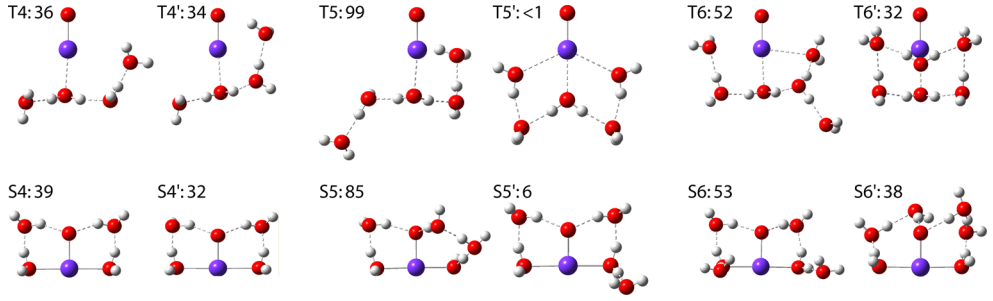

Figure 3. Molecular structures of the two most stable $AtO^+(H_2O)_n$ clusters, n = 4–6, calculated at SMD + M06-2X/mAVDZ level of theory for the triplet (top, T index) and singlet (bottom, S index) spin multiplicities. Boltzmann populations are given in percentage. Color code: magenta for At, red for O, and gray for H.

Table 1. Gibbs Free-Energy Difference (kJ mol^{-1}) Between the Singlet and Triplet $AtO^+(H_2O)_n$ Clusters, n = 4–6, Computed at Various Levels of Theory

theory	n = 4	n = 5	n = 6
M06-2X/mAVDZ	−13.3	−15.7	−40.4
SMD + M06-2X/mAVDZ	−38.0	−35.1	−53.0
SMD + 2c-M06-2X/mAVDZ	−14.1	−16.5	−22.7
SMD + 2c-(MP2//M06-2X)	−123.4	−125.9[a]	−143.7

[a]Because of convergence difficulties in the variational process of the HF calculation, T5 species has been disregarded.

reactivity is highly sensitive to SOC.[4] In order to investigate SOC contribution to the solvation of AtO^+, the structures of $AtO^+(H_2O)_n$ clusters with n = 4–6 have also been reoptimized within the SODFT framework. The two-component wave functions are variationally optimized from the previous singlet and triplet wave functions obtained by scalar-relativistic calculations. The SOC effects on the AtO^+ solvation are evidenced through the comparison of scalar-relativistic and quasirelativistic results. The clusters issued from a triplet electronic state undergo larger structural relaxations than those issued from a singlet electronic state (cf. available structures in the Supporting Information). For a given cluster size (n is fixed), the 2c-M06-2X/mAVDZ calculations stabilize more the species issued from a triplet electronic state. The free-energy gap with the species issued from a singlet electronic state is consequently reduced. (See Table 1.) Nevertheless, it was found that the clusters dominated by a Kramers-restricted closed-shell configuration, resembling a scalar-relativistic singlet, remain the most stable, and the free-energy difference increases with the size of the cluster (when n grows). This trend was verified through the explicit inclusion of SOC in ab initio calculations. The results obtained using 2c-(MP2//M06-2X) single-point energies and the bulk electrostatic contributions provided by the SMD solvation model are presented in Table 1. We notice secondly that the free-energy differences between the species issued from the singlet and triplet electronic states increase by more than 100 kJ mol^{-1}. However, we presume that this large increase is somewhat overestimated: (i) comparable disparities between scalar-relativistic M06-2X and MP2//M06-2X results are observed for $AtO^+(H_2O)_n$ clusters with n = 4–6 (see Table S1 in the Supporting Information) and (ii) scalar-relativistic CCSD(T)//M06-2X results are in better agreement with those obtained by M06-2X calculations (see Table S1 in the Supporting Information). We have verified that the disparities do not originate from an incorrect description of the interactions between water molecules by M06-2X functional or MP2 method. (See Table S2 in the Supporting Information and the related discussion.) The fact that the MP2 method destabilizes the triplet clusters with respect to the singlet ones may result from zero-order wave functions, which are far from the optimal ones, and a perturbative treatment of the electron correlation may not be sufficient. Finally, the important differences between 2c-M06-2X and 2c-(MP2//M06-2X) values reported in Table 1 prompt us to encourage the reader to focus their attention on the trends rather than on the numerical values. Therefore, it comes out that AtO^+ adopts a stable closed-shell form for its ground state. This original result allows understanding why AtO^+ readily reacts in aqueous solution with simple organic and inorganic compounds,[4,9−11] which would be spin-forbidden otherwise.

3.2. Where the Ground-State Change Is Explained.

The comparison of quasirelativistic 2c-M06-2X/mAVDZ (or 2c-(MP2//M06-2X)) calculations and scalar-relativistic M06-2X/mAVDZ (respectively, MP2//M06-2X) calculations shows that the SOC effects are moderate on the solvation of AtO^+. Spin orbit free calculations are sufficient to evidence the change of ground state for AtO^+ and to demonstrate that it mainly originates from cooperative and short-range interactions with the water molecules in the first solvation shell. This section aims at revealing the fundamentals that lead to the change of ground state. To alleviate the discussion, we have restrained the analysis to scalar-relativistic M06-2X/mAVDZ calculations. Let us consider first the approach of a water molecule in C_{2v} symmetry. The two unpaired electrons arising from the AtO^+ triplet ground state ($X^3\Sigma^-$ for the isolated ion) are distributed in one b_1 molecular orbital (MO) and one b_2 MO. The electronic density around At is almost symmetric with respect to the C_2 axis of rotation. The noncovalent interactions with the water molecule can be rationalized from the analysis of the maximum ($V_{s,max}$) of the molecular electrostatic potential (MEP) of the AtO^+ fragment. Figure 4 evidences a single maximum found along the C_2 axis at the halogen ($V_{s,max}$ = 799 kJ mol^{-1}), which is known as the "σ-hole".[28] Acting as a Lewis base, the water molecule makes attractive electrostatic interactions. The resulting cluster optimized for the triplet electronic state is therefore stabilized by halogen bonding (T1 ($^3A_2$) species in Figure 1). Regarding the first singlet exited state of the AtO^+ fragment, the HOMO is doubly occupied and belongs to the B_2 irreducible representation. The electronic density around At is stretched in the molecular plane (σ_v' bearing all AtO^+ and H_2O atoms) and the MEP exhibits a strip of highly positive electrostatic potential perpendicular to this plane. (See Figure 4.) Two maxima ($V_{s,max}$ = 816 kJ mol^{-1}) have been found on astatine surface, which are distributed on

dx.doi.org/10.1021/jp406803e | J. Phys. Chem. B 2013, 117, 10589−10595

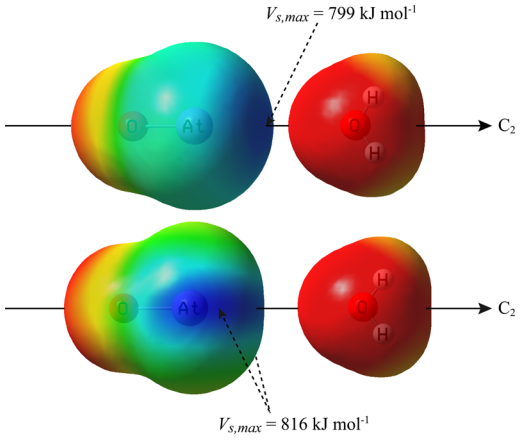

Figure 4. Molecular electrostatic potential calculated on the van der Waals surface of AtO^+ aligned with a water molecule at 5 Å (blue color indicates regions of highly positive charge). The molecular surface was defined by the 0.001 e bohr^{-3} contour of the electronic density computed at M06-2X/mAVDZ level of theory for both electronic states: triplet (top) and singlet (bottom).

either side of the σ_v' plane. To maximize the attractive electrostatic interaction with astatine, the water molecule must break the C_{2v} symmetry. Accordingly, the resulting cluster optimized for the singlet electronic state adopts a C_s molecular symmetry (S1 (^{1}A′) species in Figure 1). Note that the larger $V_{s,max}$ values for the singlet AtO^+ fragment than for triplet AtO^+ fragment indicate stronger potential interactions with the water molecule and therefore an enhanced stabilization. Note that the reliability of the MEP analysis has been verified by performing CASSCF calculations. (See Figure S1 in the Supporting Information.)

A second parameter that must be investigated during the analysis of noncovalent interactions is the charge transfer. Charge transfers can be expected from the lone pairs of the water oxygen atom to the electron-deficient At atom. If we still consider the approach of a water molecule in C_{2v} symmetry, the lone pair that had to be considered is located in one b_1 orbital (the HOMO of the isolated water molecule, see Figure 5). Regarding the AtO^+ triplet ground state, which displays a singly occupied b_1 MO, there will be a three-electron repulsive

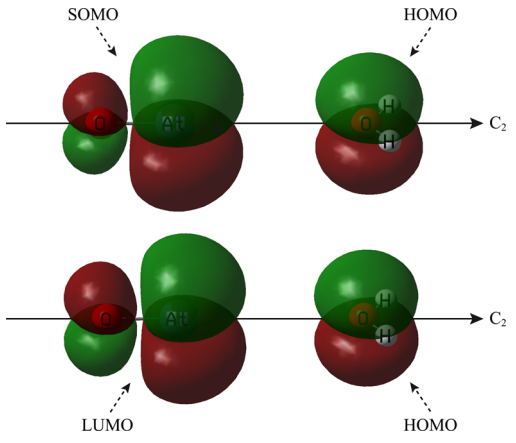

Figure 5. Frontier orbitals computed at M06-2X/mAVDZ level of theory for both the AtO^+ fragment (triplet, top, and singlet, bottom) and an aligned water molecule at 5 Å (C_{2v} symmetry). Only the orbitals that belong to the B_1 irreducible representation are shown.

interaction. This should hinder the charge transfer. The situation is completely reversed for the singlet AtO^+ fragment. The LUMO belongs to the appropriate B_1 irreducible representation and is empty: good conditions exist for charge transfer. (See Figure 5.) Note that the conditions are even more favorable when the singlet $AtO^+(H_2O)$ cluster finally adopts a C_s molecular symmetry as the orbitals bearing both water lone pairs and the AtO^+ LUMO become a′. Table 2 reports the computed partial charges for both the singlet and triplet $AtO^+(H_2O)$ clusters. The charge transfer represents 0.16 e for the singlet state that is almost three times bigger than for the triplet state. The stronger interaction with the water molecule obviously yields an added stabilization in favor of the singlet $AtO^+(H_2O)$ cluster. This is notably highlighted by the shortening of the cation−water distance: 2.366 Å instead of 2.570 Å for the triplet $AtO^+(H_2O)$ cluster. (See Figure 1.)

What comes out when a second water molecule is introduced? In terms of electrostatic interactions, the situation is less favorable for the triplet electronic state. The water molecule in the triplet $AtO^+(H_2O)$ cluster fulfills the positive σ-hole found on the MEP surface of AtO^+. (See Figure S2 in the Supporting Information.) For an added water molecule, two options are therefore possible: (i) compete with the previous water molecule to access to the σ-hole under suitable geometric conditions, which would hamper the interaction between the previous water molecule and AtO^+, and (ii) do some hydrogen bonding with the previous water molecule, which does not particularly favor the solvation of AtO^+ itself. This is evidenced by the structure displayed by the two most stable triplet $AtO^+(H_2O)_2$ clusters (T2 (^{3}A′) and T2′ (^{3}A′) species in Figure 1). In contrast, the singlet $AtO^+(H_2O)$ cluster still exhibits a free maximum on the MEP surface ($V_{s,max}$ = 733 kJ mol^{-1}, see Figure S2 in the Supporting Information) that comes from the two equivalent $V_{s,max}$ initially disclosed for the singlet AtO^+ fragment. Hence, there is a vacant place for a second water molecule that would lead to an attractive electrostatic interaction with At. The optimal molecular geometry is of C_{2v} symmetry, as displayed by the most abundant singlet $AtO^+(H_2O)_2$ cluster (S2 (^{1}A$_1$) species in Figure 1, its Boltzmann population being greater than 99%). Astatine is surrounded by three oxygen atoms that build a bent T-shape structure. This arrangement is also well-suited for charge transfers from the water molecules (some oxygen lone pairs are located in b_2 orbitals) to the electron-deficient At atom (the LUMO of the AtO^+ fragment being b_2). The total charge transfer represents 0.26 e, which is more than three times the charge transfer calculated for the most stable triplet $AtO^+(H_2O)_2$ cluster. (See Table 2.) Again, the analysis of the electrostatic interactions and charge transfers (electron delocalization) indicates for the singlet state stronger interactions between AtO^+ and the water molecules and therefore a higher stabilization.

If n is increased again, then the additional water molecules mainly act through hydrogen bonding, as shown in Figures 1 and 3. For the triplet state, they seem to not interact directly with AtO^+ but rather build a network structured by the water molecule connected to At by an halogen bond. Someone could say that the additional water molecules for the triplet clusters take place in a second solvation shell. Therefore, the charge transfers from these water molecules are found small, as shown in Table 2. In contrast, the additional water molecules are prone for the singlet state to make hydrogen bonds with the oxygen atom belonging to AtO^+. (See Figures 1 and 3.) This

dx.doi.org/10.1021/jp406803e | J. Phys. Chem. B 2013, 117, 10589−10595

Table 2. Computed Partial Charges (in e) of the Fragments Involved in the Most Stable Singlet and Triplet $AtO^+(H_2O)_n$ Clusters, $n = 1-6$[a]

	singlet							triplet						
	AtO^+	H_2O						AtO^+	H_2O					
$n = 1$	0.84	0.16						0.94	0.06					
$n = 2$	0.74	0.13	0.13					0.92	0.05	0.03				
$n = 3$	0.65	0.12	0.12	0.11				0.91	0.03	0.04	0.02			
$n = 4$	0.61	0.11	0.11	0.09	0.08			0.88	0.02	0.02	0.04	0.04		
$n = 5$	0.60	0.12	0.10	0.07	0.06	0.05		0.88	0.02	0.01	0.01	0.04	0.04	
$n = 6$	0.59	0.11	0.10	0.06	0.05	0.05	0.04	0.88	0.02	0.01	0.01	0.02	0.03	0.03

[a]Based on a natural population analysis (NPA) of the M06-2X/mAVDZ wave functions.

facilitates the electron delocalization, as illustrated by the results gathered in Table 2. Unlike the triplet clusters, the charge transfers from the additional water molecules remain important and the total charge of the AtO^+ fragment continues to decrease until $n = 6$. We suspect that the discrepancies of charge transfer between the singlet and triplet clusters are mainly responsible for the change of ground state.

Note that the greater electron delocalization discussed above for the singlet clusters allows notably rationalizing the fact that the long-range bulk effects of the solvent stabilize more the singlet clusters than the triplet ones. The latter phenomenon is obviously linked to the size of the dipole moments (and others multipolar moments). The greater electron delocalization allows for the singlet clusters magnifying their dipole moment in the presence of an external field. With six water molecules, the dipole moments of S6 and T6 clusters (see Figure 3) are, for example, 9.21 and 3.86 D, respectively, at SMD + M06-2X/mAVDZ level of theory. In fine, Figure 6 displays for the most

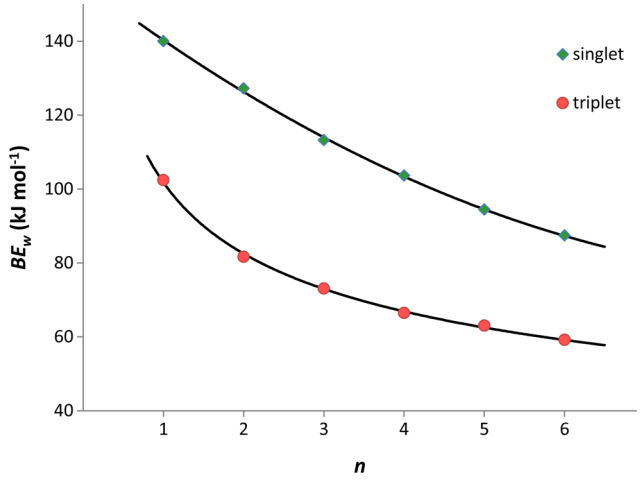

Figure 6. Evolution of the binding energy per water molecule unit, BE_w, for the singlet and triplet $AtO^+(H_2O)_n$ clusters with n increasing up to 6. The computed M06-2X/mAVDZ energies include ZPVE and BSSE corrections.

stable cluster of both spin multiplicities how the binding energy per water molecule unit, BE_w, is modified according to the number of explicit water molecules ($n = 1-6$). It is evidenced that BE_w is at least 30 kJ mol^{-1} larger for the singlet clusters than for the triplet clusters of the same size. Furthermore, BE_w decreases more rapidly for the triplet electronic state. Hence, it is ineluctable that the singlet electronic state becomes the ground state due to persistent more attractive interactions between the water molecules and AtO^+. This notably justifies limiting our investigations to $AtO^+(H_2O)_n$ clusters with $n = 1-6$ because increasing n to 7 or 8 is not expected to bring new facts that modify the fundaments governing the solvation process. The additional water molecules will mainly localize in the second solvation shell.

4. CONCLUSIONS

Using scalar and quasirelativistic quantum calculations, we have determined the stability of $AtO^+(H_2O)_n$ clusters ($n = 1-6$) for the lower states arising from the triplet and singlet spin multiplicities. An exciting property of the AtO^+ molecular ion is evidenced. While the ground state of the isolated AtO^+ and small $AtO^+(H_2O)_n$ clusters is dominated by an open-shell configuration, the larger $AtO^+(H_2O)_n$ clusters adopt a Kramers-restricted closed-shell configuration resembling to a scalar-relativistic singlet. This behavior brings to light the key role played by the water molecules of the first solvation shell. They lift up the initial degeneracy of the frontier π^* MOs in the isolated AtO^+, leading to specific interactions (electrostatic and charge transfer), which strongly favor the stabilization of the closed-shell electronic state. While some may be interested to determine the number of explicit water molecules needed to induce the ground-state change (some disparities are found between various relativistic ab initio and DFT calculations), we demonstrate that this phenomenon is ineluctable as the number of water molecules increases. Hence, AtO^+ becomes dominated in aqueous solution by a spin state of singlet character. As previously discussed,[12] this has a decisive implication because this molecular ion can therefore readily react in solution with most compounds. Another concern is related to the highly variable reproducibility reported for some astatine reactions.[3] This is commonly attributed to possible interferences with impurities due to the low amounts of astatine present. Let us recall that At is first produced in cyclotrons; then, the procedure currently involves either a direct extraction in acidic aqueous solutions or a distillation in the gas phase, followed by a condensation process in solution. As the kinetic parameters governing the conversion of the gas-phase astatine into the solvated singlet AtO^+ are unknown, we hypothesize that it may exist differences of reactivity depending on the production protocol ("wet chemistry" extraction or gas-phase distillation).

■ ASSOCIATED CONTENT

Supporting Information

Supplementary figures and tables are provided in addition to the geometries of the 12 selected clusters optimized at 2c-M06-2X/mAVDZ level of theory. This material is available free of charge via the Internet at http://pubs.acs.org.

dx.doi.org/10.1021/jp406803e | J. Phys. Chem. B 2013, 117, 10589−10595

AUTHOR INFORMATION

Corresponding Author

*E-mail: nicolas.galland@univ-nantes.fr. Tel: +33(0)2 51 12 55 71. Fax: +33(0)2 51 12 57 12.

Notes

The authors declare no competing financial interest.

ACKNOWLEDGMENTS

We thank the French National Research Agency (ANR 2010-BLAN-0807-01) and the "Region Pays de la Loire" (NUCSAN project) for financial support. This work was performed using the cluster of the PhLAM institute and HPC resources from GENCI-CINES/IDRIS (Grant 2012-c2012085117) and CCIPL (Centre de Calcul Intensif des Pays de la Loire).

REFERENCES

(1) Wilbur, D. S. [211At]astatine-Labeled Compound Stability: Issues with Released [211At]astatide and Development of Labeling Reagents to Increase Stability. *Curr. Radiopharm* **2008**, *1*, 144−176.

(2) Vaidyanathan, G.; Zalutsky, M. R. Astatine Radiopharmaceuticals: Prospects and Problems. *Curr. Radiopharm* **2008**, *1*, 177−196.

(3) Wilbur, D. S. Enigmatic Astatine. *Nat. Chem.* **2013**, *5*, 246−246.

(4) Champion, J.; Seydou, M.; Sabatie-Gogova, A.; Renault, E.; Montavon, G.; Galland, N. Assessment of an Effective Quasirelativistic Methodology Designed to Study Astatine Chemistry in Aqueous Solution. *Phys. Chem. Chem. Phys.* **2011**, *13*, 14984−14992.

(5) Pilmé, J.; Renault, E.; Ayed, T.; Montavon, G.; Galland, N. Introducing the ELF Topological Analysis in the Field of Quasirelativistic Quantum Calculations. *J. Chem. Theory Comput.* **2012**, *8*, 2985−2990.

(6) Champion, J.; Alliot, C.; Renault, E.; Mokili, B. M.; Cherel, M.; Galland, N.; Montavon, G. Astatine Standard Redox Potentials and Speciation in Acidic Medium. *J. Phys. Chem. A* **2010**, *114*, 576−582.

(7) Champion, J.; Sabatié-Gogova, A.; Bassal, F.; Ayed, T.; Alliot, C.; Galland, N.; Montavon, G. Investigation of Astatine (+III) Hydrolyzed Species: Experiments and Relativistic Calculations. *J. Phys. Chem. A* **2013**, *117*, 1983−1990.

(8) Wilbur, D. S.; Chyan, M.-K.; Nakamae, H.; Chen, Y.; Hamlin, D. K.; Santos, E. B.; Kornblit, B. T.; Sandmaier, B. M. Reagents for Astatination of Biomolecules. 6. An Intact Antibody Conjugated with a Maleimido-closo-Decaborate(2-) Reagent via Sulfhydryl Groups Had Considerably Higher Kidney Concentrations than the Same Antibody Conjugated with an Isothiocyanato-closo-Decaborate(2-) Reagent via Lysine Amines. *Bioconjugate Chem.* **2012**, *23*, 409−420.

(9) Norseyev, Y. V.; Khalkin, V. A. The Stability Constants of Chloride Complexes of Mono-Valent Astatine in Nitric Acid Solution. *J. Inorg. Nucl. Chem* **1968**, *30*, 3239−3243.

(10) Fischer, S.; Dreyer, R.; Albrecht, S. Pseudohalogen Compounds of Astatine: Synthesis and Characterization of At/I/-Tricyanomethanide-and At/I/-Azide-Compounds. *J. Radioanal. Nucl. Chem* **1987**, *117*, 275−283.

(11) Champion, J.; Alliot, C.; Huclier, S.; Deniaud, D.; Asfari, Z.; Montavon, G. Determination of Stability Constants between Complexing Agents and At(I) and At(III) Species Present at Ultra-Trace Concentrations. *Inorg. Chim. Acta* **2009**, *362*, 2654−2661.

(12) Ayed, T.; Seydou, M.; Réal, F.; Montavon, G.; Galland, N. How Does the Solvation Unveil AtO+ Reactivity? *J. Phys. Chem. B* **2013**, *117*, 5206−5211.

(13) Zhao, Y.; Truhlar, D. G. The M06 Suite of Density Functionals for Main Group Thermochemistry, Thermochemical Kinetics, Noncovalent Interactions, Excited States, And Transition Elements: Two New Functionals and Systematic Testing of Four M06-Class Functionals and 12 Other Functionals. *Theor. Chem. Acc.* **2008**, *120*, 215−241.

(14) Jacquemin, D.; Perpéte, E. A.; Ciofini, I.; Adamo, C. Assessment of Functionals for TD-DFT Calculations of Singlet−Triplet Transitions. *J. Chem. Theory Comput.* **2010**, *6*, 1532−1537.

(15) Peterson, K. A.; Figgen, D.; Goll, E.; Stoll, H.; Dolg, M. Systematically Convergent Basis Sets with Relativistic Pseudopotentials. II. Small-Core Pseudopotentials and Correlation Consistent Basis Sets for the Post-d Group 16−18 Elements. *J. Chem. Phys.* **2003**, *119*, 11113−11123.

(16) Dunning, T. H., Jr. Gaussian Basis Sets for Use in Correlated Molecular Calculations. I. The Atoms Boron through Neon and Hydrogen. *J. Chem. Phys.* **1989**, *90*, 1007−1023.

(17) Kendall, R. A.; Dunning, T. H., Jr.; Harrison, R. J. Electron Affinities of the First-Row Atoms Revisited. Systematic Basis Sets and Wave Functions. *J. Chem. Phys.* **1992**, *96*, 6796−6806.

(18) Werner, H.-J.; Knowles, P. J.; Knizia, G.; Manby, F. R.; Schütz, M.; Celani, P.; Korona, T.; Lindh, R.; Mitrushenkov, A.; Rauhut, G. et al. *MOLPRO*, version 2012.1; A package of ab initio programs, 2012. http://www.molpro.net.

(19) Bischoff, F. A.; Klopper, W. Second-Order Electron-Correlation and Self-Consistent Spin-Orbit Treatment of Heavy Molecules at the Basis-Set Limit. *J. Chem. Phys.* **2010**, *132*, 094108.

(20) Straatsma, T. P.; Aprà, E.; Windus, T. L.; Bylaska, E. J.; de Jong, W.; Hirata, S.; Valiev, M.; Hackler, M.; Pollack, L.; Harrison, R. et al. *NWChem, A Computational Chemistry Package for Parallel Computers*, version 5.1.1; Pacific Northwest National Laboratory: Richland, WA, 2008.

(21) Choi, Y. J.; Lee, Y. S. Spin-Orbit Density Functional Theory Calculations for Heavy Metal Monohydrides. *J. Chem. Phys.* **2003**, *119*, 2014−2019.

(22) Cho, W. K.; Choi, Y. J.; Lee, Y. S. Spin-Orbit Density Functional Theory Calculations for IX (X = F, Cl, Br and I) Molecules. *Mol. Phys.* **2005**, *103*, 2117−2122.

(23) *TURBOMOLE*, v6.3.1, a development of University of Karlsruhe and Forschungszentrum Karlsruhe; TURBOMOLE: Karlsruhe, Germany, 2011.

(24) Marenich, A. V.; Cramer, C. J.; Truhlar, D. G. Universal Solvation Model Based on Solute Electron Density and on a Continuum Model of the Solvent Defined by the Bulk Dielectric Constant and Atomic Surface Tensions. *J. Phys. Chem. B* **2009**, *113*, 6378−6396.

(25) Mantina, M.; Chamberlin, A. C.; Valero, R.; Cramer, C. J.; Truhlar, D. G. Consistent van der Waals Radii for the Whole Main Group. *J. Phys. Chem. A* **2009**, *113*, 5806−5812.

(26) Frisch, M. J.; Trucks, G. W.; Schlegel, H. B.; Scuseria, G. E.; Robb, M. A.; Cheeseman, J. R.; Scalmani, G.; Barone, V.; Mennucci, B.; Petersson, G. A. et al..; *Gaussian 09*, revision A.02; Gaussian, Inc.: Wallingford, CT, 2009.

(27) A detailed investigation of the AtO^+ spectrum will be reported in a forthcoming article.

(28) Politzer, P.; Lane, P.; Concha, M.; Ma, Y.; Murray, J. An overview of halogen bonding. *J. Mol. Model.* **2007**, *13*, 305−311.